Acta Crystallographica Section F
Structural Biology and Crystallization Communications
ISSN 1744-3091

Flexibility of the P-loop of Pim-1 kinase: observation of a novel conformation induced by interaction with an inhibitor

Lorien J. Parker,[a] Hisami Watanabe,[a] Keiko Tsuganezawa,[a] Yuri Tomabechi,[a] Noriko Handa,[a] Mikako Shirouzu,[a] Hitomi Yuki,[a] Teruki Honma,[a] Naoko Ogawa,[a] Tetsuo Nagano,[b] Shigeyuki Yokoyama[a,c,d]* and Akiko Tanaka[a,b]*

[a]RIKEN Systems and Structural Biology Center, 1-7-22 Suehiro-cho, Tsurumi, Yokohama 230-0045, Japan, [b]Open Innovation Center for Drug Discovery, The University of Tokyo, 7-3-1 Hongo, Bunkyo-ku, Tokyo 113-0033, Japan, [c]Laboratory of Structural Biology, Graduate School of Science, The University of Tokyo, 7-3-1 Hongo, Bunkyo-ku, Tokyo 113-0033, Japan, and [d]Department of Biophysics and Biochemistry, Graduate School of Science, The University of Tokyo, 7-3-1 Hongo, Bunkyo-ku, Tokyo 113-0033, Japan

Correspondence e-mail: yokoyama@biochem.s.u-tokyo.ac.jp, aktanaka@riken.jp

Received 20 April 2012
Accepted 15 June 2012

PDB References: Pim-1, complex with compound **1**, 3umx; complex with compound **2**, 4eny; complex with compound **3**, 4enx.

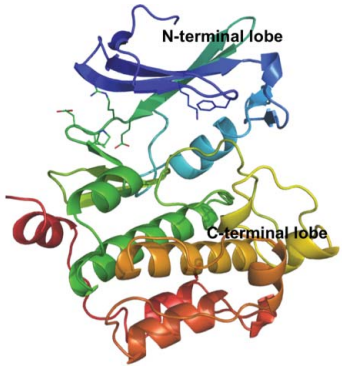

The serine/threonine kinase Pim-1 is emerging as a promising target for cancer therapeutics. Much attention has recently been focused on identifying potential Pim-1 inhibitor candidates for the treatment of haematopoietic malignancies. The outcome of a rational drug-design project has recently been reported [Nakano *et al.* (2012), *J. Med. Chem.* **55**, 5151–5156]. The report described the process of optimization of the structure–activity relationship and detailed from a medicinal chemistry perspective the development of a low-potency and non-selective compound initially identified from *in silico* screening into a potent, selective and metabolically stable Pim-1 inhibitor. Here, the structures of the initial *in silico* hits are reported and the noteworthy features of the Pim-1 complex structures are described. A particular focus was placed on the rearrangement of the glycine-rich P-loop region that was observed for one of the initial compounds, (*Z*)-7-(azepan-1-ylmethyl)-2-[(1*H*-indol-3-yl)methylidene]-6-hydroxy-1-benzofuran-3(2*H*)-one (compound **1**), and was also found in all further derivatives. This novel P-loop conformation, which appears to be stabilized by an additional interaction with the β3 strand located above the binding site, is not usually observed in Pim-1 structures.

1. Introduction

Pim-1, a member of the serine/threonine kinase family, is a proto-oncogene and its overexpression is involved in prostate, pancreas and colon cancers, acute myeloid leukaemia (AML) and other haematopoietic malignancies (Amson *et al.*, 1989; Cibull *et al.*, 2006; Dhanasekaran *et al.*, 2001).

Pim-1 participates in a signal cascade downstream of the receptor-type tyrosine kinase Flt-3, which has also been actively investigated as a promising therapeutic target for AML (Kiyoi & Naoe, 2002). Pim-1 phosphorylates proteins related to cell proliferation, such as Bad (Ser112; Yan *et al.*, 2003; Aho *et al.*, 2004), c-Myc (Mochizuki *et al.*, 1997), SOCS (Chen *et al.*, 2002) and p27kip1 (Morishita *et al.*, 2008).

The kinase domain of Pim-1 shares 61 and 76% amino-acid identity with Pim-2 and Pim-3, respectively (Brault *et al.*, 2010). Pim-1 and Pim-3 are highly expressed in hepatic and pancreatic cancer cells, while Pim-2 is predominant in haematological and prostate cancer cells (Brault *et al.*, 2010). It has not been determined whether the Pim-family kinases have functional redundancy and thus whether a non-isozyme specific inhibitor would produce unwanted and unexpected side effects. Although Pim-1, Pim-2 and Pim-3 knockout mice show no adverse side effects, Pim-1-deficient mice show a lower level of CXCR4 expression, which is not compensated by Pim-2 (Grundler *et al.*, 2009).

The β-strand-rich N-terminal lobe and the predominantly α-helical C-terminal lobe are connected by a hinge region (Leu120, Glu121, Arg122 and Pro123) in which the ATP-binding pocket is located (Fig. 1). The hinge residues are the targets of ATP-mimetic inhibitors, while non-mimetics (Pogacic *et al.*, 2007; Qian *et al.*, 2009; Kumar *et al.*, 2005; Jacobs *et al.*, 2005) often bind on the opposite side of the ATP pocket and do not form the characteristic hydrogen bond with Glu121.

The glycine-rich P-loop (Gly45, Ser46, Gly47, Gly48, Phe49, Gly50, Ser51 and Val52) forms a roof on the ATP-pocket (Fig. 1). It is flexible and has been implicated in determining the specificity, selectivity and affinity of inhibitors *via* induced-fit binding modes (Kumar *et al.*, 2005). In the apoprotein structure (Qian *et al.*, 2005; PDB entry 1xqz), Phe49 of the P-loop is tucked into the binding pocket, forming a lid on the binding site (Fig. 2*a*). When AMP-PNP is bound (Qian *et al.*, 2005; PDB entry 1xr1) Phe49 is displaced by its phosphates and is shifted by more than 10 Å from its location in the apo structure (Fig. 2*b*). This 'flipped-out' conformation has also been observed in other Pim-1 complexes (Cheney *et al.*, 2007; Tao *et al.*, 2009; López-Ramos *et al.*, 2010; Nishiguchi *et al.*, 2011). The displacement of the P-loop is considered to affect the overall binding energies of different ligands (Doudou *et al.*, 2010).

To the best of our knowledge, despite the deposition of over 63 structures of Pim-1–inhibitor/substrate complexes, there are no Pim-1 inhibitors in advanced stages of clinical investigation. We believe that inhibitors such as compound **1** (Fig. 3*a*) and its derivatives described in Nakano *et al.* (2012) have the potential to be developed further. Compound **14**, the most advanced of the series, inhibits the growth of the human leukaemia cell line MV4-11 (Nakano *et al.*, 2012). Like compound **1** and its derivatives, binding of **14** caused the P-loop to adopt a novel conformation. Since this rearrangement was first observed with compound **1**, it is representative of all subsequent

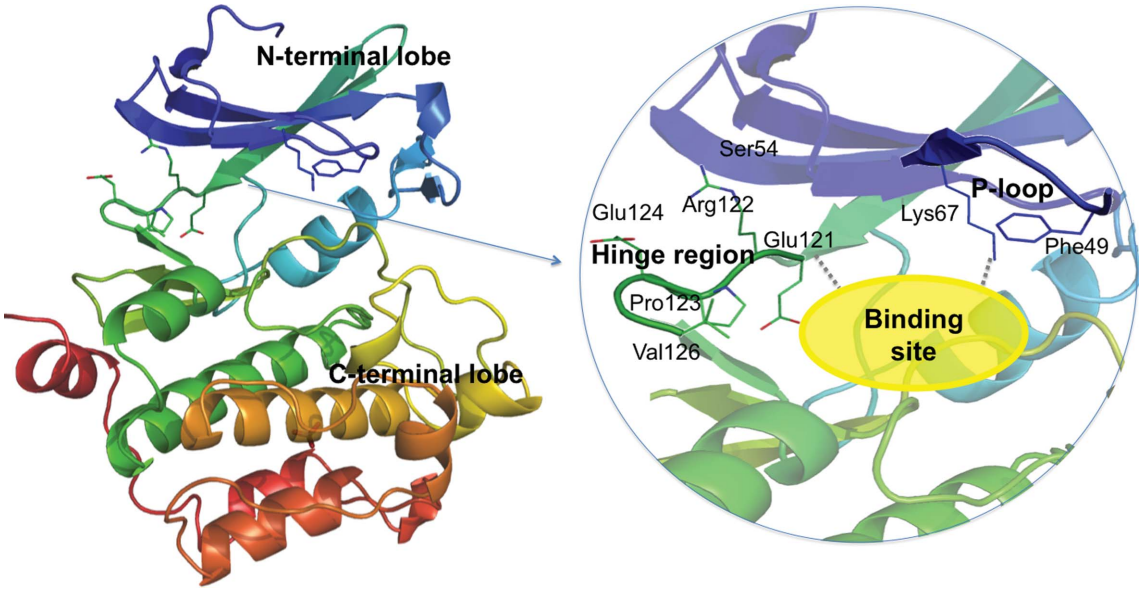

Figure 1
Pim-1 kinase hinge region and P-loop. The overall tertiary structure of Pim-1 kinase is shown on the left in a cartoon format, with each secondary-structure element coloured using a rainbow scheme. The N-terminal lobe is at the top and the α-helical C-terminal lobe is at the bottom. A close-up view of the binding-site region (in the yellow oval) is shown on the right. The hinge region is shown on the left in green. Residues Glu121, Arg122, Pro123, Glu124 and Val126 are depicted as stick models. Ser54, at the end of the P-loop, is also highlighted. The interaction with Glu121 which is usually formed by mimetics is depicted by a dashed line. The P-loop is shown on the right side of the binding site in dark blue. Residues Phe49 and Lys67 are highlighted. The dashed line denotes the common interaction with Lys67.

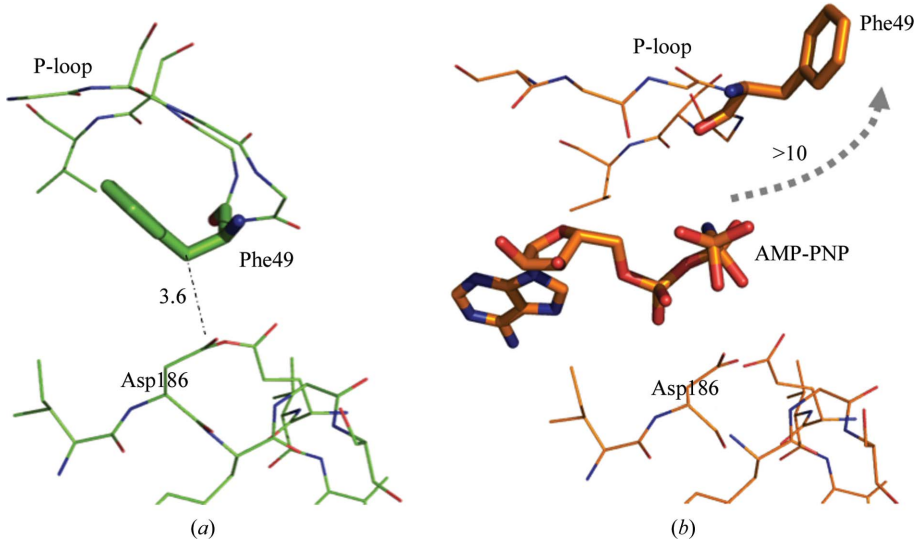

Figure 2
Comparison of the P-loop conformations in the apo and AMP-PNP-bound forms. (*a*) The apo structure, (*b*) the AMP-PNP-bound structure (Qian *et al.*, 2005; PDB entry 1xr1). The compounds and the Phe49 residue are depicted with thick sticks. The grey dashed line depicts the shift in the position of the Phe49 residue in the AMP-PNP complex compared with its position in the apo form. The distance is given in angstroms.

derivative structures that bind in the same binding site (structures not shown) and thus is described in detail here.

2. Materials and methods

2.1. *In silico* screening

In silico screening was performed as reported previously (Tsuganezawa *et al.*, 2012). One of the hit compounds, (*Z*)-7-(azepan-1-ylmethyl)-2-[(1*H*-indol-3-yl)methylidene]-6-hydroxy-1-benzofuran-3(2*H*)-one, is investigated here (compound **1**). In an alternative screening strategy, PDB entries 1yxt (Kumar *et al.*, 2005) and 2bzh (Debreczeni *et al.*, 2006) were selected for docking experiments. A total of 702 potential compounds were selected. Among these, two additional compounds, (2*E*,5*Z*)-2-(2-chlorophenylimino)-5-(4-hydroxy-3-methoxybenzylidene)thiazolidin-4-one and (2*E*,5*Z*)-2-(2-chlorophenylimino)-5-(4-hydroxy-3-nitrobenzylidene)thiazolidin-4-one, inhibited Pim-1 kinase activity by more than 85% at a final concentration of 10 µmol and were investigated further. These two compounds, **2** and **3**, respectively (IC_{50} = 0.089 and 0.550 µ*M*, respectively), and that from the first screen, compound **1** (IC_{50} = 0.24), are shown in Fig. 3(*a*). One of the derivatives, (*Z*)-6-benzyloxy-2-[(1*H*-indol-3-yl)methylidene]-7-[(piperazin-1-yl)methyl]-1-benzofuran-3(2*H*)-one, (compound **9**), and the most advanced compound, (*Z*)-2-[(1*H*-indazol-3-yl)methylidene]-6-methoxy-7-[(piperazin-1-yl)methyl]-1-benzofuran-3(2*H*)-one (compound **14**), are also shown for reference (Nakano *et al.*, 2012).

2.2. Pim-1 expression and purification for crystallization

The kinase domain of human Pim-1 was synthesized by the *Escherichia coli* cell-free system using the dialysis method (Kigawa *et al.*, 2004, 2007; Matsuda *et al.*, 2007). Details of the purification and expression methods have been reported previously (Nakano *et al.*, 2012).

2.3. Pim-1 crystallization

Human Pim-1 was crystallized under the conditions previously reported by Jacobs *et al.* (2005). Soaking involved the addition of the solid compound in a well solution containing 3% DMSO for 24 h. The use of the soaking method to determine the crystal structure is considered to be appropriate and has been used by other groups for Pim-1-inhibitor analyses (Schulz *et al.*, 2011). This decision was supported by the observation that the binding-site region and the P-loop of Pim-1 are flexible in the preformed crystal and can adjust

Table 1
Data-collection and refinement statistics.

Values in parentheses are for the highest resolution bin.

	Compound **1**	Compound **2**	Compound **3**
Data collection			
Temperature (K)	100	100	100
Space group	$P6_5$	$P6_5$	$P6_5$
Unit-cell parameters			
a (Å)	98.21	96.77	97.07
b (Å)	98.21	96.77	97.07
c (Å)	80.88	80.96	80.94
Resolution (Å)	85.13–2.55 (2.62–2.55)	31.67–2.80 (2.95–2.80)	31.78–2.80 (2.95–2.80)
No. of observations	83622 (121560)	134525 (19422)	244424 (35368)
No. of unique reflections	14489 (2099)	10721 (1555)	10791 (1565)
Data completeness (%)	99.4 (98.9)	100 (100)	99.9 (100)
R_{merge}†	0.074 (0.40)	0.079 (0.40)	0.086 (0.39)
$\langle I/\sigma(I)\rangle$	8.3 (1.9)	9.2 (1.9)	8.5 (2.0)
Multiplicity	5.8 (5.8)	12.5 (12.5)	22.7 (22.6)
Refinement			
No. of non-H atoms			
Protein	2122	2148	2160
Compound	29	24	25
Solvent (H_2O)	112	60	55
Resolution (Å)	2.55	2.8	2.8
R_{cryst}‡ (%)	17.7	17.26	19.02
R_{free}§ (%)	22.9	22.36	23.26
Reflections used in *R*-factor calculations			
Number	14485	10689	10762
Completeness (%)	99.4	100	99.93
R.m.s.d.s from ideal geometry			
Bonds (Å)	0.020	0.005	0.006
Angles (°)	1.99	0.777	0.891
Mean *B* (Å^2)			
Protein			
Main chain	37.64	42.98	43.32
Side chain	38.69	46.97	44.07
Solvent	40.16	31.37	30.75
Compound	37.59	37.07	32.38
Ramachandran plot, residues in (%)			
Most favoured regions	95.1	98.03	98.09
Disallowed regions	0.0	0.0	0.0
PDB code	3umx	4eny	4enx

† $R_{merge} = \sum_{hkl}\sum_i |I_i(hkl) - \langle I(hkl)\rangle|/\sum_{hkl}\sum_i I_i(hkl)$, where $I_i(hkl)$ is the intensity of the *i*th measurement of an equivalent reflection with indices *hkl*. ‡ $R_{cryst} = \sum_{hkl} ||F_{obs}| - |F_{calc}||/\sum_{hkl} |F_{obs}|$, where F_{obs} and F_{calc} are the observed and calculated structure-factor amplitudes, respectively. § R_{free} was calculated using 5% of the diffraction data that were selected randomly and not used throughout refinement.

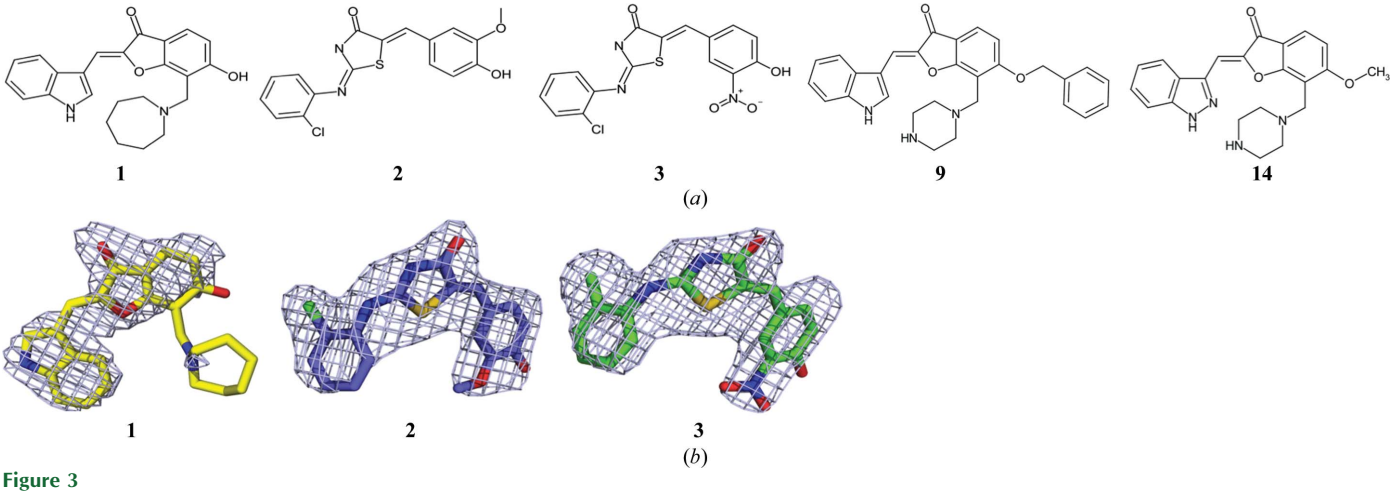

Figure 3
Chemical structures and electron density. (*a*) Chemical structures of compounds **1**, **2**, **3**, **9** and **14**. (*b*) The electron densities of compounds **1**, **2** and **3** are represented as blue meshes calculated as OMIT $F_o - F_c$ maps contoured at 3σ.

their positions to accommodate inhibitor binding. Crystals from the same drop exhibited very different P-loop conformations depending on which compound was used for soaking or, conversely, if no compounds were used at all (apo), despite being harvested from the same well and having the same crystal contacts. We thus concluded that any structural changes that we observed in the compound-bound structures compared with the apo crystal harvested from the same drop were a consequence of interactions between the protein and the ligand. Crystals were cryoprotected with 30% glycerol and flash-cooled in liquid nitrogen. Data were collected either in-house on a Rigaku R-AXIS IV++ detector or on the BL26B1 or BL41XU beamlines at SPring-8, Harima, Japan. Data from an apo crystal grown in the same drop were also collected as a control. The apo crystal had an almost identical structure to PDB entry 1xqz (Qian *et al.*, 2005) and thus is not discussed in detail here.

2.4. Pim-1 structure solution

MOSFLM was employed for processing and integration (Leslie, 1992) and *SCALA* was used for scaling (Winn *et al.*, 2011). *Phaser* (McCoy *et al.*, 2007) was used for molecular replacement with PDB entry 3a99 (Morishita *et al.*, 2011) as a model. The space group is $P6_5$ and there is one molecule in the asymmetric unit. Refinement was performed using *REFMAC* (Winn *et al.*, 2011; Murshudov *et al.*, 2011) for the complexes with compound **1** and its derivatives and *PHENIX* (Adams *et al.*, 2010) for the complexes with compounds **2** and **3**. Model building was accomplished with *Coot* (Emsley & Cowtan, 2004).

2.5. Accession numbers

The coordinates and structure factors of the complexes have been deposited in the PDB with accession codes 3umx, 4eny and 4enx for compounds **1**, **2** and **3**, respectively.

3. Results

3.1. X-ray structures

The crystals of the complexes of Pim-1 with compounds **1**, **2** and **3** diffracted to 2.55, 2.8 and 2.8 Å resolution, respectively. These values are lower than those for the complexes with compound **1** derivatives, for which a positive correlation between resolution and affinity/ADMET properties was observed, and resolutions as good as 1.95 Å were achieved for some of the better inhibitors (data not shown). The electron densities for the compounds were immediately evident in the $F_o - F_c$ and $2F_o - F_c$ maps (Fig. 3*b*). Compounds **1**, **2** and **3** were fitted with occupancies of 80, 90 and 82%, respectively, and average *B* factors of 37.6, 37.1 and 32.44 Å^2, respectively. The average protein *B* factors were 37.6, 43.0 and 43.3 Å^2 for the main-chain atoms and 38.7, 47.0 and 44.1 Å^2 for the side-chain atoms, respectively. Data statistics are presented in Table 1.

The structures of the complexes with compound **1** derivatives all superimposed with r.m.s.d.s of between 0.24 and 0.41 for 260 residues using secondary-structure matching with *Coot* (Emsley & Cowtan, 2004), even in the vicinity of the binding site.

The azepine ring of compound **1**, which points towards the peptide-binding site between residues Asp128 and Glu171, has poorly resolved electron density (Fig. 3*b*), reflecting the mobility of this group owing to the lack of protein interactions. Correspondingly, these *B* factors are high (average of 60 Å^2), while those in the ordered indole group (average of 21 Å^2) are low. The complexes of compounds **1**, **2** and **3** all adopt a classic Pim-1 binding mode, although the interaction between the P-loop and compound **1** differs from that usually observed.

3.2. Conformation of the P-loop

In the complexes with compounds **2** and **3** (Figs. 4*a* and 4*b*) the P-loop is displaced compared with the apo form (Fig. 2*a*). The Phe49 side chain has rotated and now points out from the binding site in the opposite direction to that observed in the apo structure. A similar movement is also observed in other Pim-1 structures complexed with either AMP-PNP (PDB entries 1xr1, 3a99 and 1yxt; Qian *et al.*, 2005; Morishita *et al.*, 2011; Kumar *et al.*, 2005) or inhibitors (PDB entries 2obj and 3jyo; Cheney *et al.*, 2007; Tao *et al.*, 2009). The binding of compound **1** also induced a conformational shift of the P-loop (Fig. 4*c*). In this structure, however, the entire P-loop has been raised, increasing the volume of the binding site compared with the apo structure (Figs. 2*a* and 4*c*). Unlike the structures of the complexes with compounds **2** and **3**, the Phe49 side chain, which is raised by 3.7 Å compared with the apo form, still points towards the binding site without being twisted or rotated. In this conformation the P-loop makes two notable interactions specific to the compound **1** complex: (i) it stacks against the dihydrobenzofuranone core of the inhibitor

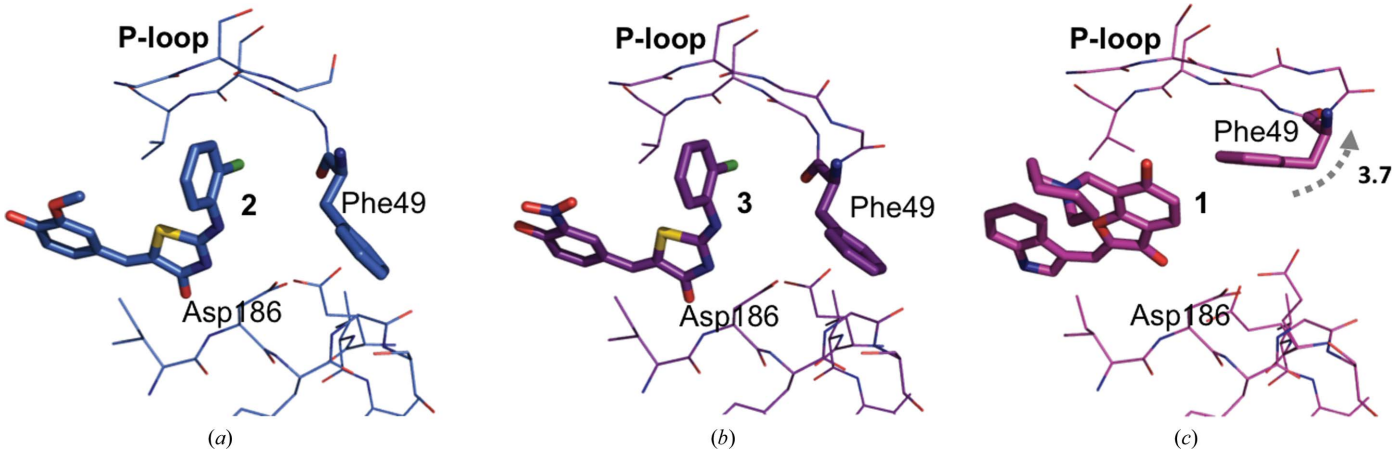

Figure 4
Comparison of the P-loop conformations in (*a*) the complex with compound **2**, (*b*) the complex with compound **3** and (*c*) the complex with compound **1**. The compounds and the Phe49 residue are depicted by thick sticks. The grey dashed line depicts the shift in position of the Phe49 residue in the compound **1** complex compared with its position in the apo form. The distance is given in angstroms.

(Fig. 5*a*) and (ii) it exhibits an additional interaction between the main chain of Phe49 and the main chain of Glu70 in the β3 strand located above it (described below). An identical P-loop conformation was also observed in the compound **1** derivatives that were introduced in Nakano *et al.* (2012) but are not described in detail here owing to limited space.

3.3. Inhibitor–protein interactions

The interactions between compound **1** and the protein were briefly described in Nakano *et al.* (2012). Notably, unlike compounds **2** or **3**, compound **1** (and its derivatives) form a hydrogen bond to the hinge residue, Glu121, which is typical of ATP-mimetic inhibitors (Fig. 5*b*).

Compounds **2** and **3** bind to Pim-1 in almost identical manners (Fig. 6). They form hydrogen-bonding interactions with Lys67 at the back of the ATP-binding site through the N atom of the thiazolidine group. The chloro moiety of the chlorobenzene group forms long-range interactions with the P-loop through Gly50. Neither the guaiacol group of compound **2** nor the nitrophenoxy group of compound **3** make any direct interactions with the protein.

4. Discussion

4.1. Inhibitor–protein interactions

In recent years, more than 63 Pim-1–inhibitor structures have been described, pinpointing many important interactions that influence their specificity and potency.

Compounds **1**, **2** and **3** form some of these essential interactions with the Pim-1 protein. They form hydrogen bonds with the catalytically essential Lys67 (Friedmann *et al.*, 1992) and longer interactions with Asp186. All three compounds also form water-mediated inter-

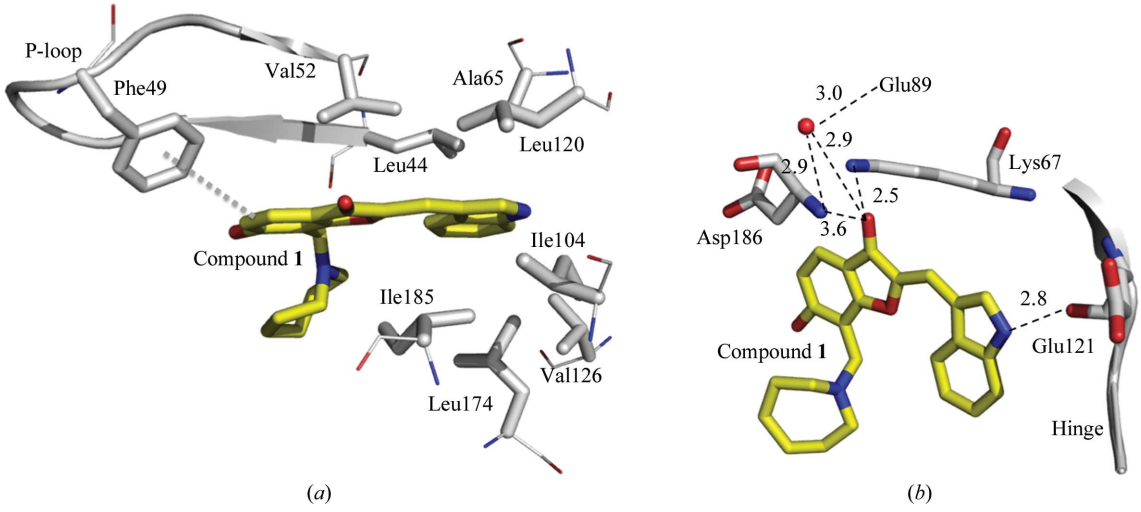

Figure 5
Interactions between compound **1** and Pim-1 kinase. The C atoms of compound **1** are represented by yellow sticks and the protein residues are coloured grey. N and O atoms are coloured blue and red, respectively. A water molecule is displayed as a red sphere. Bonds are drawn as dashed lines and distances are given in angstroms. (*a*) shows the hydrophobic interactions between the protein and the compound and (*b*) shows the hydrophilic interactions.

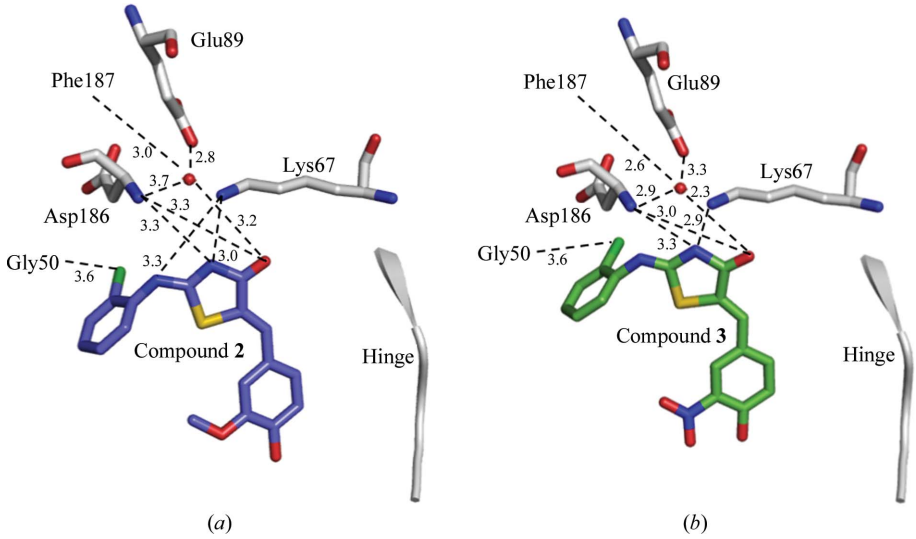

Figure 6
(*a*) Direct interactions between compound **2** and Pim-1 kinase. The C atoms of the protein residues and the compound are represented by grey and blue sticks, respectively. N and O atoms are coloured blue and red, respectively, S atoms are coloured yellow and Cl atoms are coloured bright green. A water molecule is shown as a red sphere. The bonds are drawn as dashed lines and the distances are given in angstroms. (*b*) Direct interactions between compound **3** and Pim-1 kinase. Atoms are coloured as in (*a*). A water molecule is shown as a red sphere. Bonds are drawn as dashed lines and distances are given in angstroms. The backbone of the hinge region, residues 120–123, is shown in grey for reference.

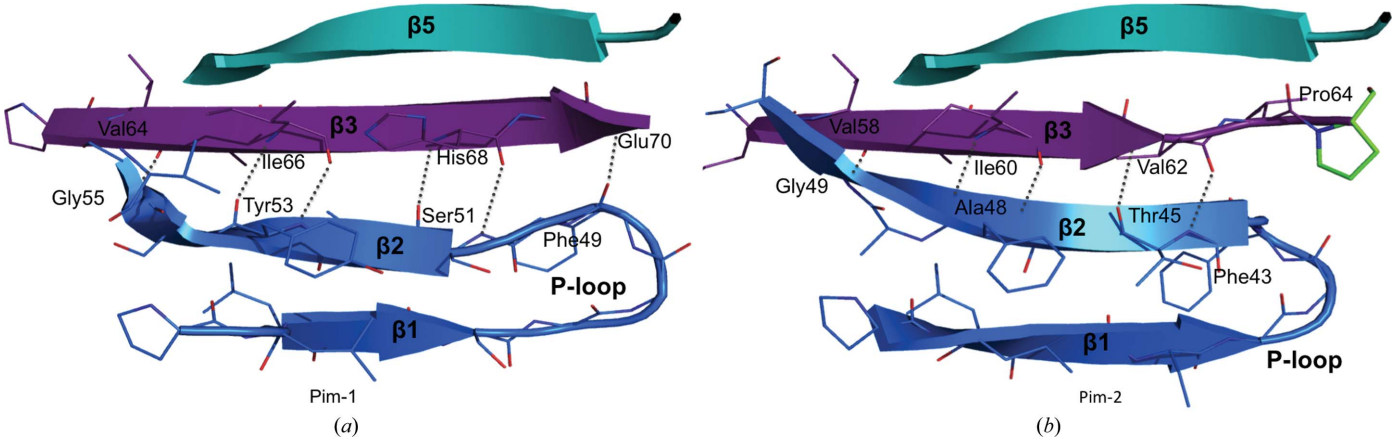

Figure 7
Novel conformation of the P-loop stabilized by interactions with the β3 loop lying above it. Hydrogen bonds between the backbone residues of the β3 and β2 strands are depicted by dotted lines. In the Pim-1–compound **1** complex (*a*) a hydrogen bond is formed between Glu70 and Phe49. In Pim-2 (*b*), however, the residue at position 70 is proline instead of glutamate so this bond is not formed. Therefore, the conformation adopted by the P-loop in Pim-1 is unlikely to occur in Pim-2.

actions with Glu89 and either Asp186 or Phe187. These residues are critical for protein stability by maintaining the position of the regulatory spine region (López-Ramos *et al.*, 2010) and the Lys67/Glu89/Asp186 salt bridge/triad (Qian *et al.*, 2005). Lys67 is highly conserved, forming a salt bridge with the α-phosphate of ATP (Qian *et al.*, 2005). Mutation of Lys67 results in the abolition of Pim-1 kinase activity (Friedmann *et al.*, 1992).

Compound **1** interacts directly with Glu121 (Fig. 5*b*), which usually forms a critical hydrogen bond to the imide NH group of the bound ATP (Qian *et al.*, 2005). Interactions with Glu121 and Lys67 are common characteristics of kinase frequent hitters (Aronov & Murcko, 2004), but only a handful of compounds actually make both classical interactions simultaneously (PDB entries 2bzj, 2o3p, 2o64, 2o65, 3bwf and 3dcv; Debreczeni *et al.*, 2006; Holder *et al.*, 2007; Maksimoska *et al.*, 2008; Shafer *et al.*, 2008). Thus, both of these interactions were maintained throughout our inhibitor-development process (Nakano *et al.*, 2012).

The C atoms in the benzofuranone core of compound **1** stack with the aromatic residue Phe49, presumably stabilizing not only the compound binding but also the conformation of the P-loop (Fig. 5*a*). These hydrophobic interactions are not observed in the complexes with compounds **2** and **3** owing to the rotation of the Phe49 side chain (Figs. 4*a* and 4*b*).

Compound **1** and its derivatives form hydrophobic interactions with Ala65, Ile104, Leu120, Leu174, Ile185 and the P-loop residue Leu44 (Fig. 5*a*). In Pim-1, Leu174 plays a significant role in selectivity, since it is commonly replaced by a cysteine, a serine or an alanine in other kinases. Val52 and Ala65, which are located directly above the position where the adenine ring of ATP normally binds, are usually involved in hydrophobic interactions with nucleotides (Kornev *et al.*, 2006). These residues presumably play a similar role in binding compound **1**.

4.2. P-loop conformation

As mentioned above, the most interesting feature of the compound **1** complex is the conformation of the P-loop. Superposition of compound **1** on the apo form reveals that the dihydrobenzofuran core of **1** and the Phe49 side chain in the apo form would clash, explaining why the P-loop has readjusted. If Phe49 had been flipped out, as in the structures of the compound **2** and **3** complexes, then neither the additional hydrogen bond to the β3 strand nor the hydrophobic stacking with the compound would have been possible. The structures of the derivatives adopt the same P-loop conformation as the parent compound **1** (unpublished data). Only compound **9**, which has a benzyl substitution on the benzofuran-3-one core, was not successfully crystallized, presumably owing to a clash with the P-loop and resultant structural flexibility.

Superpositions of the 58 Pim-1–inhibitor complexes submitted to the PDB using secondary-structure matching in *Coot* (Emsley & Cowtan, 2004) revealed that only three other inhibitors, β-carboline ligand I (PDB entry 3cxw; Huber *et al.*, 2012), β-carboline ligand II (PDB entry 3cy2; Huber *et al.*, 2012) and one of the 3*H*-benzo[4,5]-thieno[3,2-d]pyrimidin-4-one inhibitors (PDB entry 3jxw; Tao *et al.*, 2009), also raise the P-loop. However, the conformation in compound **1** has the closest proximity to the β3 strand. Here, the main chain of Phe49 in the P-loop forms an additional bond to Glu70 in the β3 strand (Fig. 7*a*), which is part of a rigid β-sheet formed by five β-strands in the N-lobe. The β2 strand (Gly50–Val58) and the β3 strand (Asn61–Lys71) pack together through pairs of interactions which are formed in almost all Pim-1 structures. Usually, after Ser51 the P-loop peels off and heads away from the β3 strand towards the ATP-binding site below. Interestingly, in the compound **1** structure, in which this loop is raised, an additional interaction is formed. This extra interaction cannot exist in the other complexes owing to the distance between the P-loop and Glu70, even for 3cwx, 3cy2 and 3jxw (Tao *et al.*, 2009). We postulate that this extra bond may stabilize the flexible P-loop and participate in the selectivity of these compounds, which all prefer Pim-1 over Pim-2 (Nakano *et al.*, 2012). It could be hypothesized that this hydrogen bond cannot be formed in Pim-2 since the residue at position 70 is a proline (Fig. 7*b*).

The Pim kinase hinge conformation is unique and is held in place by a network of polar interactions. The Val126 residue, which forms part of the hydrophobic pocket, interacts with Pro123 (Fig. 1). The side chain of Arg122 is sandwiched between the side chains of Glu124 and Ser54, forming a network of bonds that reinforce the conformation of the hinge. In Pim-2, however, Glu124 is replaced by leucine and an alanine replaces Ser54 and Val126. As a result, Arg122 is disordered in Pim-2, presumably affecting the hinge dynamics (Bullock *et al.*, 2009), while the Val-to-Ala substitution in Pim-2 at position 126 probably contributes to reducing the overall hydrophobicity of the site, thus producing a higher desolvation energy (Tao

et al., 2009). The overall hydrophobicity of the Pim-2 binding site is indeed less than that of Pim-1. Together, these factors may also explain the selectivity for Pim-1 over Pim-2 observed for compound 1 and its derivatives (data not shown). Further investigations are needed to further explore these hypotheses.

5. Concluding remarks

We have recently shown that our rational optimization strategy can successfully be employed to improve both potency and selectivity. The identification of compound **1** and its subsequent evolution into the improved compound **14** provide proof of concept.

Structural studies of this series, from the parent compound (reported here) through to the final compound (reported recently in Nakano *et al.*, 2012), provide insights into how increased potency and selectivity can be achieved for this kind of Pim-1 inhibitor. We believe that the conformation adopted by the P-loop in response to the binding of these compounds contributes to the characteristics displayed by these inhibitors. In the next phase of our drug-design strategy we hope to continue to improve these inhibitors to develop a compound that is delivered effectively, shows anticancer properties and is truly specific for Pim-1.

This work was supported in part by the Targeted Protein Research Programs from the Ministry of Education, Culture, Sports, Science and Technology of Japan. We thank the staff of BL41XU at SPring-8 for their kind assistance with data collection. LJP was supported by a National Health and Medical Research Council of Australia (NHMRC) C. J. Martin Overseas Postdoctoral Fellowship.

References

Adams, P. D. *et al.* (2010). *Acta Cryst.* D**66**, 213–221.
Aho, T. L., Sandholm, J., Peltola, K. J., Mankonen, H. P., Lilly, M. & Koskinen, P. J. (2004). *FEBS Lett.* **571**, 43–49.
Amson, R., Sigaux, F., Przedborski, S., Flandrin, G., Givol, D. & Telerman, A. (1989). *Proc. Natl Acad. Sci. USA*, **86**, 8857–8861.
Aronov, A. M. & Murcko, M. A. (2004). *J. Med. Chem.* **47**, 5616–5619.
Brault, L., Gasser, C., Bracher, F., Huber, K., Knapp, S. & Schwaller, J. (2010). *Haematologica*, **95**, 1004–1015.
Bullock, A. N., Russo, S., Amos, A., Pagano, N., Bregman, H., Debreczeni, J. É., Lee, W. H., von Delft, F., Meggers, E. & Knapp, S. (2009). *PLoS One*, **4**, e7112.
Chen, X. P., Losman, J. A., Cowan, S., Donahue, E., Fay, S., Vuong, B. Q., Nawijn, M. C., Capece, D., Cohan, V. L. & Rothman, P. (2002). *Proc. Natl Acad. Sci. USA*, **99**, 2175–2180.
Cheney, I. W., Yan, S., Appleby, T., Walker, H., Vo, T., Yao, N., Hamatake, R., Hong, Z. & Wu, J. Z. (2007). *Bioorg. Med. Chem. Lett.* **17**, 1679–1683.
Cibull, T. L., Jones, T. D., Li, L., Eble, J. N., Baldridge, L. A., Malott, S. R., Luo, Y. & Cheng, L. (2006). *J. Clin. Pathol.* **59**, 285–288.
Debreczeni, J. É., Bullock, A. N., Atilla, G. E., Williams, D. S., Bregman, H., Knapp, S. & Meggers, E. (2006). *Angew. Chem. Int. Ed. Engl.* **45**, 1580–1585.
Dhanasekaran, S. M., Barrette, T. R., Ghosh, D., Shah, R., Varambally, S., Kurachi, K., Pienta, K. J., Rubin, M. A. & Chinnaiyan, A. M. (2001). *Nature (London)*, **412**, 822–826.
Doudou, S., Sharma, R., Henchman, R. H., Sheppard, D. W. & Burton, N. A. (2010). *J. Chem. Inf. Model.* **50**, 368–379.
Emsley, P. & Cowtan, K. (2004). *Acta Cryst.* D**60**, 2126–2132.
Friedmann, M., Nissen, M. S., Hoover, D. S., Reeves, R. & Magnuson, N. S. (1992). *Arch. Biochem. Biophys.* **298**, 594–601.
Grundler, R. *et al.* (2009). *J. Exp. Med.* **206**, 1957–1970.
Holder, S., Zemskova, M., Zhang, C., Tabrizizad, M., Bremer, R., Neidigh, J. W. & Lilly, M. B. (2007). *Mol. Cancer Ther.* **6**, 163–172.
Huber, K., Brault, L., Fedorov, O., Gasser, C., Filippakopoulos, P., Bullock, A. N., Fabbro, D., Trappe, J., Schwaller, J., Knapp, S. & Bracher, F. (2012). *J. Med. Chem.* **55**, 403–413.
Jacobs, M. D., Black, J., Futer, O., Swenson, L., Hare, B., Fleming, M. & Saxena, K. (2005). *J. Biol. Chem.* **280**, 13728–13734.
Kigawa, T., Matsuda, T., Yabuki, T. & Yokoyama, S. (2007). *Cell-Free Protein Synthesis Methods and Protocols*, edited by A. S. Spirin & J. R. Swartz, pp. 83–97. Weinheim: Wiley-VCH.
Kigawa, T., Yabuki, T., Matsuda, N., Matsuda, T., Nakajima, R., Tanaka, A. & Yokoyama, S. (2004). *J. Struct. Funct. Genomics*, **5**, 63–68.
Kiyoi, H. & Naoe, T. (2002). *Leuk. Lymphoma*, **43**, 1541–1547.
Kornev, A. P., Haste, N. M., Taylor, S. S. & Ten Eyck, L. F. (2006). *Proc. Natl Acad. Sci. USA*, **103**, 17783–17788.
Kumar, A., Mandiyan, V., Suzuki, Y., Zhang, C., Rice, J., Tsai, J., Artis, D. R., Ibrahim, P. & Bremer, R. (2005). *J. Mol. Biol.* **348**, 183–193.
Leslie, A. G. W. (1992). *Jnt CCP4/ESF–EACBM Newsl. Protein Crystallogr.* **26**.
López-Ramos, M., Prudent, R., Moucadel, V., Sautel, C. F., Barette, C., Lafanechère, L., Mouawad, L., Grierson, D., Schmidt, F., Florent, J.-C., Filippakopoulos, P., Bullock, A. N., Knapp, S., Reiser, J.-B. & Cochet, C. (2010). *FASEB J.* **24**, 3171–3185.
Maksimoska, J., Williams, D. S., Atilla-Gokcumen, G. E., Smalley, K. S., Carroll, P. J., Webster, R. D., Filippakopoulos, P., Knapp, S., Herlyn, M. & Meggers, E. (2008). *Chemistry*, **14**, 4816–4822.
Matsuda, T., Koshiba, S., Tochio, N., Seki, E., Iwasaki, N., Yabuki, T., Inoue, M., Yokoyama, S. & Kigawa, T. (2007). *J. Biomol. NMR*, **37**, 225–229.
McCoy, A. J., Grosse-Kunstleve, R. W., Adams, P. D., Winn, M. D., Storoni, L. C. & Read, R. J. (2007). *J. Appl. Cryst.* **40**, 658–674.
Mochizuki, T., Kitanaka, C., Noguchi, K., Sugiyama, A., Kagaya, S., Chi, S., Asai, A. & Kuchino, Y. (1997). *Oncogene*, **15**, 1471–1480.
Morishita, D., Katayama, R., Sekimizu, K., Tsuruo, T. & Fujita, N. (2008). *Cancer Res.* **68**, 5076–5085.
Morishita, D., Takami, M., Yoshikawa, S., Katayama, R., Sato, S., Kukimoto-Niino, M., Umehara, T., Shirouzu, M., Sekimizu, K., Yokoyama, S. & Fujita, N. (2011). *J. Biol. Chem.* **286**, 2681–2688.
Murshudov, G. N., Skubák, P., Lebedev, A. A., Pannu, N. S., Steiner, R. A., Nicholls, R. A., Winn, M. D., Long, F. & Vagin, A. A. (2011). *Acta Cryst.* D**67**, 355–367.
Nakano, H., Saito, N., Parker, L. J., Tada, Y., Abe, M., Tsuganezawa, K., Yokoyama, S., Tanaka, A., Kojima, H., Okabe, T. & Nagano, T. (2012). *J. Med. Chem.* **55**, 5151–5156.
Nishiguchi, G. A., Atallah, G., Bellamacina, C., Burger, M. T., Ding, Y., Feucht, P. H., Garcia, P. D., Han, W., Klivansky, L. & Lindvall, M. (2011). *Bioorg. Med. Chem. Lett.* **21**, 6366–6369.
Pogacic, V., Bullock, A. N., Fedorov, O., Filippakopoulos, P., Gasser, C., Biondi, A., Meyer-Monard, S., Knapp, S. & Schwaller, J. (2007). *Cancer Res.* **67**, 6916–6924.
Qian, K. *et al.* (2009). *J. Med. Chem.* **52**, 1814–1827.
Qian, K. C., Wang, L., Hickey, E. R., Studts, J., Barringer, K., Peng, C., Kronkaitis, A., Li, J., White, A., Mische, S. & Farmer, B. (2005). *J. Biol. Chem.* **280**, 6130–6137.
Schulz, M. N., Fanghänel, J., Schäfer, M., Badock, V., Briem, H., Boemer, U., Nguyen, D., Husemann, M. & Hillig, R. C. (2011). *Acta Cryst.* D**67**, 156–166.
Shafer, C. M., Lindvall, M., Bellamacina, C., Gesner, T. G., Yabannavar, A., Jia, W., Lin, S. & Walter, A. (2008). *Bioorg. Med. Chem. Lett.* **18**, 4482–4485.
Tao, Z.-F. *et al.* (2009). *J. Med. Chem.* **52**, 6621–6636.
Tsuganezawa, K. *et al.* (2012). *J. Mol. Biol.* **417**, 240–252.
Winn, M. D. *et al.* (2011). *Acta Cryst.* D**67**, 235–242.
Yan, B., Zemskova, M., Holder, S., Chin, V., Kraft, A., Koskinen, P. J. & Lilly, M. (2003). *J. Biol. Chem.* **278**, 45358–45367.